JCIS Open 12 (2023) 100098

Contents lists available at ScienceDirect

JCIS Open

journal homepage: www.journals.elsevier.com/jcis-open

# Antibacterial composites based on halloysite with silver nanoparticles and polyoxometalates

Adeliya R. Sayfutdinova [a], Kirill A. Cherednichenko [a], Alexey A. Bezdomnikov [b], Ubirajara Pereira Rodrigues-Filho [c], Vladimir V. Vinokurov [a], Berik Tuleubayev [d], Denis Rimashevskiy [a], Dmitry S. Kopitsyn [a], Andrei A. Novikov [a,*]

[a] Gubkin University, Moscow, 119991, Russian Federation
[b] Frumkin Institute of Physical Chemistry and Electrochemistry RAS, Moscow, 119071, Russian Federation
[c] Institute of Chemistry of São Carlos, University of São Paulo, São Carlos, 13560-970, São Paulo, Brazil
[d] NCJSC "Medical University of Karaganda", Karaganda, 100008, Kazakhstan

ARTICLE INFO

*Keywords:*
Heteropolyacids
Halloysite
*S. aureus*
*P. aeruginosa*
*A. baumannii*

ABSTRACT

The spread of bacterial infections aggravated by the development of microbial resistance to antibiotics requires the creation of protective antibacterial materials. Nanomaterials with biocides can provide antibacterial and antibiofilm properties against Gram-positive and Gram-negative bacteria. In this work, we synthesized nanocomposites with silver nanoparticles and different polyoxometalates of Keggin-structure (phosphomolybdic, phosphotungstic, and tungstosilicic acids) on eco-friendly nanoclay called halloysite. We found that the nanocomposite containing silver nanoparticles and phosphomolybdic acid deposited on the halloysite possesses the best antibacterial performance of all the obtained composites, having a minimal inhibitory concentration of 0.5 g/L against *S. aureus*, 0.25 g/L against *P. aeruginosa* and *A. baumannii*. This composite reduces the viability of formed biofilms at a concentration of 2.5 g/L.

## 1. Introduction

The development and spread of new infections lead to the resistance of bacterial strains to existing antibiotics and antiseptics. In pandemic time, the problem of bacterial resistance is particularly challenging [1, 2]. Advances in material chemistry must be employed as a passive method of antibacterial protection along with the active method that is based on pharmaceuticals. Material components, particularly biocides, should provide both antimicrobial and antibiofilm properties to reduce the risk of bacterial contamination.

One of the most common biocides used to obtain antibacterial nanomaterials is silver. It is considered that silver electrostatically interacts with bacterial membranes, leading to destabilization and/or destruction of the cell wall and blocking the respiratory chain [3–5]. Colloid silver synthesized using aqueous leaf extracts showed antibacterial and antibiofilm activity against MRSA (methicillin-resistant *S. aureus)*, *P. aeruginosa*, *H. influenzae*, and *S. pneumoniae*. MBEC (minimal biofilm eradication concentration) for some MRSA and *P. aeruginosa* strains can reach 22–44 ppm and 3 ppm correspondingly [6]. Another study on AgNPs green synthesis reports biofilm inhibition activity of the best sample against pathogenic bacteria *S. aureus, P. aeruginosa, B. subtilis*, and *E. coli* that is 85.00 %, 78.81 %, 73.04 %, and 66.69 % [7]. The strength of biofilm produced by multidrug-resistant *A. baumannii* influences the action of AgNPs. The growth of weak and moderate biofilm producers was more inhibited by nanoparticles than that of strong biofilm producers. The percentage (assessed by the optical density of crystal violet-stained biofilms) of preformed *A. baumannii* biofilms treated with AgNPs were 85 ± 12 %, 77 ± 15 %, and 51 ± 11 %, respectively [8].

To reduce the risk of developing implant-associated infections (IAI), multicomponent surfaces with introduced AgNPs were created. Biomimetic orthopedic titanium-based coating with AgNPs/gentamicin-embedded silk fibroin showed significant inhibition of *S. aureus* growth, adhesion, and biofilm formation [9]. Polymer coating was designed consisting of hydroxyapatite film with immobilized ionic silver

* Corresponding author. 65/1 Leninsky Prospect, Moscow, 119991, Russian Federation.
*E-mail addresses:* sayfutdinova.a@gubkin.ru (A.R. Sayfutdinova), cherednichenko.k@gubkin.ru (K.A. Cherednichenko), bezdomnikovaa@phyche.ac.ru (A.A. Bezdomnikov), ubirajara@usp.br (U.P. Rodrigues-Filho), vladimir@vinokurov.me (V.V. Vinokurov), tuleubaev@qmu.kz (B. Tuleubayev), drimashe@gmail.com (D. Rimashevskiy), kopicin.d@inbox.ru (D.S. Kopitsyn), novikov.a@gubkin.ru (A.A. Novikov).

https://doi.org/10.1016/j.jciso.2023.100098
Received 29 June 2023; Received in revised form 21 October 2023; Accepted 28 October 2023
Available online 30 October 2023
2666-934X/© 2023 Published by Elsevier B.V. This is an open access article under the CC BY-NC-ND license (http://creativecommons.org/licenses/by-nc-nd/4.0/).

**Abbreviations**

| | |
|---|---|
| MRSA | Methicillin-resistant *Staphylococcus aureus* |
| MSSA | Methicillin-susceptible *Staphylococcus aureus* |
| IAI | implant-associated infections |
| AgNPs | silver nanoparticles |
| MBEC | minimal biofilm eradication concentration |
| POM | polyoxometalate |
| PMA | phosphomolybdic acid |
| PTA | phosphotungstic acid |
| STA | tungstosilicic acid |
| TEM | transmission electron microscopy |
| HNT | halloysite nanotubes |
| EDX | Energy-dispersive X-ray Fluorescence analysis |
| PTFE | polytetrafluoroethylene |
| HNT-Ag | halloysite nanotubes with silver nanoparticles |
| HNT-Ag-PMA | halloysite nanotubes with silver nanoparticles and phosphomolybdic acid |
| HNT-Ag-PTA | halloysite nanotubes with silver nanoparticles and phosphotungstic acid |
| HNT-Ag-STA | halloysite nanotubes with silver nanoparticles and tungstosilicic acid |
| MIC | minimum inhibitory concentration |

via inositol hexaphosphate chelation onto polyether ether ketone. Silver-coated surface provide both antibacterial purity and antibiofilm properties *in vitro* and *in vivo* [10].

The antibacterial activity of AgNPs can be improved by their combination with polyoxometalates (POM). Polyoxometalates particularly heteropolyanions of Keggin-structure are a well-known class of inorganic nanoclusters of various sizes and compositions. Due to their wide range of physical and chemical properties, POM are actively used in, e. g., catalysis, photochemistry, electrochemistry, and medicine [11]. AgNPs modified with phosphomolybdic acid (PMA) and phosphotungstic acid (PTA) possess high antibacterial activity against Gram-positive *S. albus* and Gram-negative *E. coli* as compared to unmodified AgNPs [12]. Self-sterilizing hybrid phosphotungstate ormosils loaded with AgNPs showed complete eradication of *S. aureus* and *P. aeruginosa* [13]. Nanocomposite based on reduced graphene oxide with AgNPs and PMA is effective against *E. coli*, and characterized by minimum inhibitory concentration equal to 0.256 g/L [14]. Therefore, the combination of silver and POM have the potential for controlling Gram-positive and Gram-negative bacteria spreading.

Treatments against mature bacterial biofilms were recently studied employing AgNPs embedded in Pluronic F127 hydrogel [15] and POM-polypeptide complexes [16]. Despite the large number of studies dedicated to the antibacterial silver-containing composites, we could not find any published results on the antibiofilm activity of silver nanoparticles combined with heteropolyacids, except for the semi-quantitative crystal violet staining assay that showed mild efficacy of AgNPs/PTA-PDA-loaded hydrogel scaffold against *S. aureus* (40 % growth reduction) and *E. coli* (45 % growth reduction) biofilms in the dark [17]. Thus, the quantitative study of the antibiofilm activity of AgNPs combined with heteropolyacids is novel and highly desirable.

Porous carriers such as halloysite, sepiolite, and zeolite can be used as supports for bactericides [18–20]. Halloysite nanotubes (HNT) are widely used as a nanocarrier for AgNPs due to their tubular structure and chemically active external and internal surfaces and are suitable for antibacterial formulations [21–25]. In our previous study [26], we obtained halloysite-based nanocomposite with AgNPs and PMA having a minimum inhibitory concentration of 0.50 g/L for Gram-positive *S. aureus* and Gram-negative *P. aeruginosa* and 0.25 g/L for *A. baumannii*. The porous structure of HNT provides a prolonged release of PMA for about 2 h after contact with water (see Fig. 3 in Ref. [26]). The synthesis technique was multistage including preliminary silanization of HNT followed by deposition of the pre-synthesized AgNPs and impregnation of PMA.

In this work, we aimed to simplify the method of nanocomposite production. We synthesized AgNPs on HNTs *in situ* and loaded the composites with various POMs. Furthermore, for the first time to our knowledge, we systematically studied various POMs (phosphomolybdic, phosphotungstic, and tungstosilicic acid) loaded into HNTs in combination with AgNPs and compared their action against mature bacterial biofilms. We found that the combination of porous tubular carrier, silver nanoparticles, and encapsulated phosphomolybdic acid reduces the viability of mature bacterial biofilms for more than four orders of magnitude.

## 2. Experimental section

### 2.1. Materials

Halloysite nanotubes (HNTs) and silver nitrate (99.8 %) were purchased from Sigma-Aldrich (St. Louis, MO, USA). Phosphomolybdic acid hydrate (80 %), phosphotungstic acid hydrate, and tungstosilicic acid hydrate were purchased from Acros Organics (USA). Mueller–Hinton broth and Mueller–Hinton agar were purchased from Becton Dickinson (USA). Ethanol (96 %), heptane, and agarose were purchased from Chimmed (Russia).

### 2.2. Methods

#### 2.2.1. Synthesis of halloysite based silver/POM nanocomposites

Halloysite nanotubes without any modification were dispersed in 0.1 M silver nitrate ethanol solution, kept for 1 h with magnetic stirring, centrifuged at 4000 g, and dried at 70 °C overnight. Then the obtained sample was placed in 0.01 M ethanol solution of the corresponding POM for 2 h, centrifuged, and dried at 70 °C.

#### 2.2.2. Composites characterization

Morphology of AgNPs onto halloysite nanotubes before and after treatment with polyoxometalates were investigated by Transmission electron microscopy (TEM) and Energy-dispersive X-ray spectroscopy (EDX). 5 μL of sample dispersion in heptane was dropped on a carbon/formvar TEM grid (Ted Pella, Redding, CA, USA) and dried at room temperature. TEM micrographs were obtained using a JEM-2100 electron microscope (JEOL, Japan) at an accelerating voltage of 200 kV. Elemental distribution over the samples was determined by the JED-2300 (JEOL, Japan) analysis station. The particle size distribution was calculated by TEM-image analysis using ImageJ software. Analysis of particle size distribution was performed by measurement of more than 500 particles.

#### 2.2.3. Antibacterial assay

Clinical isolates of strain *Staphylococcus aureus (MSSA)* ATCC 29213, *Pseudomonas aeruginosa* RES-2352, and *Acinetobacter baumannii* MAR14-2675 were kindly provided by the Institute of Antimicrobial Chemotherapy (Smolensk, Russia). Antibacterial studies were carried out in 96-well microplates using broth microdilution as described in Ref. [26]. Each well was filled with 100 μL of the sample suspension and 100 μL of inoculum in Mueller–Hinton broth (with a bacterial density equal to $1.5 \times 10^6$ CFU/mL). The resulting concentration of composite was 1.00, 0.50, and 0.25 g/L. Microplates were incubated at 37 °C for 18 h. Material from each well was seeded using serial 10-fold dilution series on Mueller–Hinton agar. After incubation, the bacterial colonies were counted, and growth inhibition was determined. All experiments in microplates were repeated by three independent experiments.

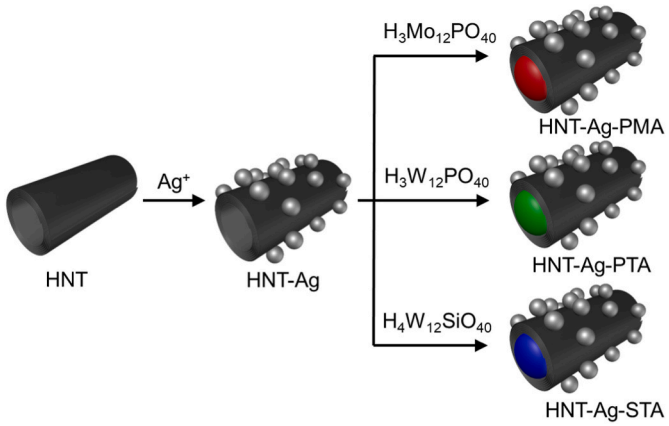



**Fig. 1.** Scheme of synthesis of the studied materials.

### 2.2.4. *Biofilm eradication assay*

Biofilm eradication assay (antibiofilm activity) was performed by using 96-well microplates according to Ref. [27]. For *in vitro* cultivation of biofilms, 4 × 4 × 4 mm polytetrafluoroethylene (PTFE) cubes were placed in wells inoculated with 150 μL of bacterial suspension (with a bacterial density equal to $1.5 \times 10^5$ CFU/mL) and then the microplate was incubated in an orbital shaker at 35 °C and 110 rpm for 20 h. The cubes with preformed biofilms were transferred to the wells of the microplate with 200 μL of nanocomposite suspension and incubated for 18 h. The control cubes with preformed biofilm were placed in a liquid medium without the presence of a nanocomposite. To determine the effect of nanocomposite on biofilm viability the biofilms were destroyed by ultrasound (Elmasonic, 37 kHz with power output of 200 W) as described in Ref. [13]. No effect of sonication on the number of surviving cells was found. The dispersed biofilms were recultivated on nutrient agar, and the number of colony units was counted.

## 3. Results and discussions

Phosphomolybdic acid (PMA), phosphotungstic acid (PTA), and tungstosilicic acid (STA) were used as polyoxometalates (POM). The scheme of synthesis of the studied materials is presented in Fig. 1. At the first stage, nanocomposite with halloysite and silver nanoparticles (HNT-Ag) was obtained with AgNPs of 2.6 ± 0.9 nm diameter formed inside and outside the halloysite nanotubes (Fig. 2). The obtained HNT-Ag was then loaded with various POMs.

After the treatment of the HNT-Ag nanocomposite with the corresponding POM, particle size has increased, and particle size distribution has broadened depending on the POM used. This effect may be explained by the incomplete reduction of silver nitrate by ethanol during deposition and drying or by the Ostwald ripening of AgNPs in the presence of POM. The nanocomposites containing AgNPs and POM were labeled as HNT-Ag-PMA, HNT-Ag-PTA, and HNT-Ag-STA. The morphology of nanocomposites and particle size distribution are shown in Fig. 2.

Typically, the preparation of halloysite-based antibacterial composites requires pre-modification of halloysite with amino silanes, which is a time-consuming operation. We focused on simplifying the obtaining method while aiming to achieve good antibacterial properties. In the first step, the halloysite was loaded with silver ions from ethanol solution and dried (at 70 °C) with subsequent treatment with POM ethanol solution. After treatment of HNT-Ag with POM, AgNPs have enlarged (from 2.6 to 3.8 nm). The increase in silver particle size after modification with phosphomolybdic acid was also observed earlier [26]. It is known that the heteropolyanions adsorb on the surface of silver and gold nanoparticles in acid solutions due to the coordination of polyoxometalate oxygen atoms to an ordered outer layer of metal atoms [28, 29] and under certain conditions are used as both reducing and stabilizing agents of noble metal nanoparticles [30,31]. In the series of obtained nanocomposites, the widest particle size distribution is typical for the composite with PTA.

According to a literature review, drying of HNT loaded with $AgNO_3$ plays a key role in the formation of AgNPs on the nanotube surface [32]. The following treatment of the obtained composite with POM leads to the further nucleation or Ostwald ripening of AgNPs. Increasing of drying temperature of silver ion loaded halloysite to 100 °C resulted in larger nanoparticles on the surface and their morphological parameters then did not change upon treatment with POM solution. Therefore, the presence of small nucleated AgNPs favored their subsequent interaction with POM.

Since individual molecules of polyoxometalates adsorbed on AgNPs cannot be identified in TEM/STEM modes of JEOL JEM-2100 UHR, the presence of polyoxometalates was proved with EDX and the corresponding elemental analysis. Fig. 3 demonstrates EDX-mapping performed for Ag/POM antibacterial composites. The concentrations of the main elements in POM-based nanocomposites are shown in Table S1 in the Supplementary material.

As shown in Fig. 3, silver occurs as individual nanoparticles in the scanning area. The presence of molybdenum/tungstic is observed throughout the scanning region, with the maximum intensity occurring on halloysite nanotubes. The treatment of the HNT-Ag composite in the POM solution should also lead to sorption of the heteropolyanion not only on the silver and halloysite surfaces but also inside of the tubes due to electrostatic interactions. It is worth noting that the dynamics of heteropolyacid release from halloysite agree with the size of Keggin polyoxometalates (circa 1 nm) and halloysite lumen (15–20 nm); the

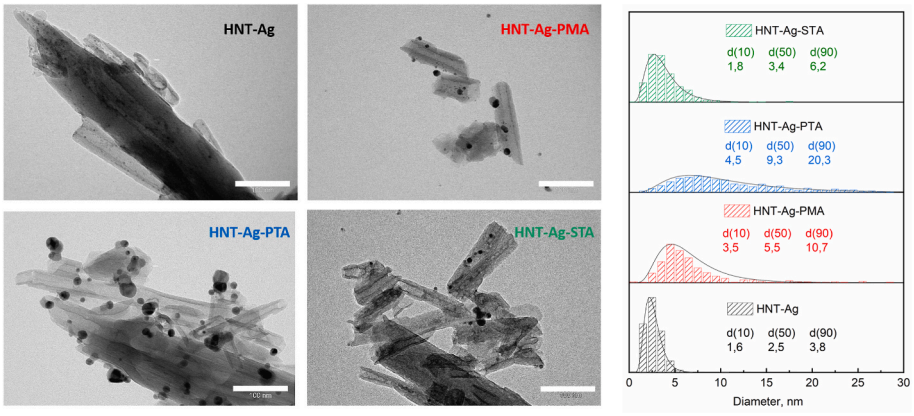



**Fig. 2.** Morphology of nanocomposites. TEM-images (scale bar is 100 nm). Particle size distribution and percentile values of nanoparticles on HNT-Ag, HNT-Ag-PMA, HNT-Ag-PTA, HNT-STA nanocomposites.

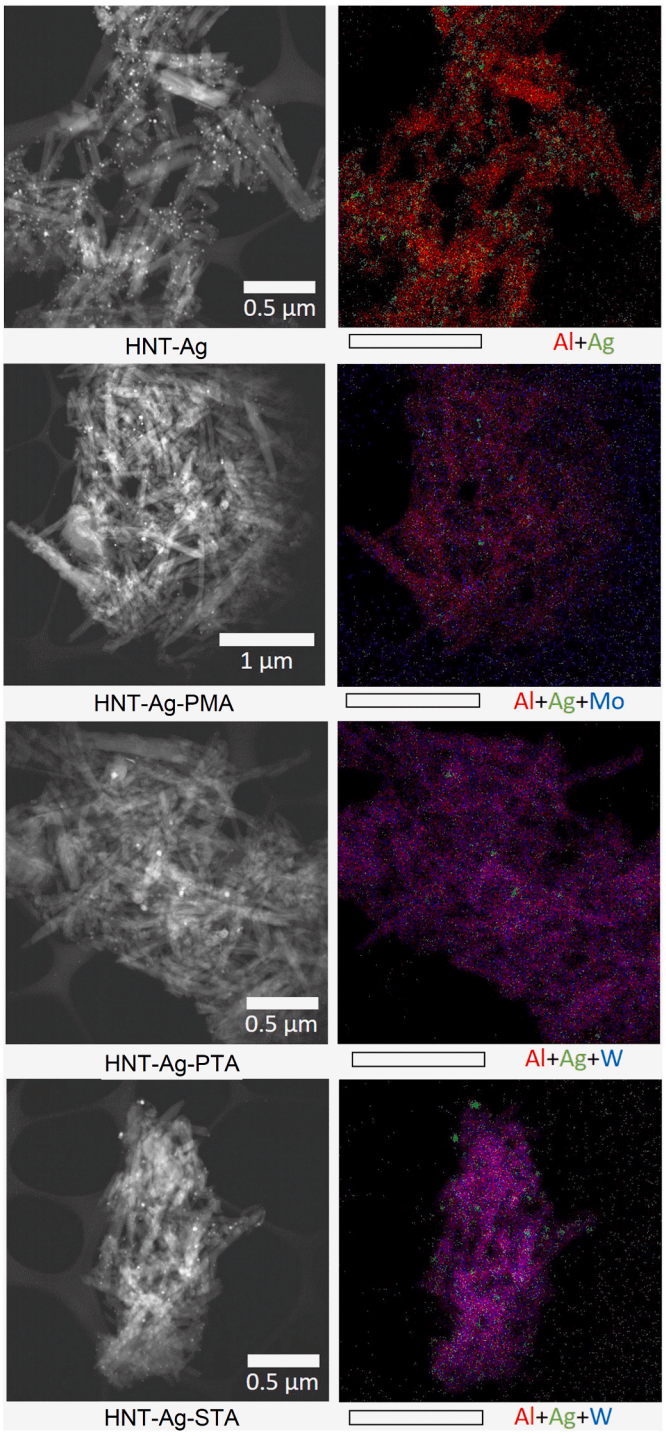



**Fig. 3.** STEM images and EDX-mapping of HNT-Ag, HNT-Ag-PMA, HNT-Ag-PTA, HNT-Ag-STA (Al – red color, Ag – green color, Mo, W – blue color, the resulting purple color indicates the colocalization of Al and Mo or W). (For interpretation of the references to color in this figure legend, the reader is referred to the Web version of this article.)

release dynamics was described by a Korsmeyer-Peppas model [33] with an exponent parameter of 0.4174, indicative of low screening [26].

We used the HR-TEM approach to elucidate the nature of silver-containing particles in the obtained composites. The HR-TEM images of AgNPs are shown in Fig. 4.

As shown in Fig. 4, the silver-containing particles in all studied samples were revealed as AgNPs with (111) interatomic distances of 2.36 Å. Neither in TEM-EDX nor in HR-TEM images, we did not observe silver nitrate or $Ag_2O$ particles. The apparent absence of silver nitrate or $Ag_2O$ in the HNT-Ag sample favors the hypothesis that the silver nitrate was completely reduced by ethanol, and the Ag particle size evolution is the Ostwald ripening induced by the POM addition.

The chosen procedure allows for obtaining a POM-silver-based composite with improved antibacterial properties. *S. aureus, P. aeruginosa,* and *A. baumannii* cause many nosocomial infections [34], therefore, we chose these strains as model bacterial cultures. Quantitative studies in the microplates demonstrated that the antibacterial properties of nanocomposites at a concentration equal to 1.00 g/L decrease in the series HNT-Ag-PMA ≈ HNT-Ag-PTA>HNT-Ag-STA>HNT-Ag (Fig. 5).

The percentage of growth suppression of *S. aureus*, *P. aeruginosa*, and *A. baumannii* by HNT-Ag are 35, 49, and 46 %. The nanocomposite with STA acts only slightly better than HNT-Ag. Nanocomposites with PMA and PTA completely suppress the growth of all bacteria. The minimum inhibitory concentrations (MIC), determined for HNT-Ag-PMA and HNT-Ag-PTA are 0.50 and 1.00 g/L towards *S. aureus*, and 0.25 and 0.50 g/L as to *P. aeruginosa*, *A. baumannii* (Table 1).

We can see from Table 1 that HNT-Ag-PMA and HNT-Ag-PTA composites have remarkably higher antibacterial action than either individual PMA or AgNPs on various carriers in the absence of POM. Furthermore, the low antibacterial efficiency of AgNPs alone prevents precise determination of MIC in many published studies [17,37]. The best composite in this work (HNT-Ag-PMA) has a MIC comparable to that of the AgNPs and PMA deposited onto reduced graphene oxide (Ag/PMA/RGO) [14].

The antibacterial action of POM-based nanocomposites is attributed to their ability to destroy the bacterial cell wall, leading to the leakage of intracellular substances [11]. In the presence of silver, POM may serve as an oxidant and as a redox catalyst, facilitating the oxidation of AgNPs to silver ions. Furthermore, all tested POMs are strong acids [38,39] and may accelerate the silver ions release by acidifying the water medium, thus intensifying the antibacterial action of the composites.

Individual Keggin-type POMs demonstrate the antibacterial action *in vitro* that decreases in the row PMA > PTA » STA [40], thus differing from their relative acidity that decreases in the row PTA > STA > PMA [41,42]. We observed the same PMA > PTA » STA ordering of POM-based AgNPs composites by their antibacterial action as for individual POMs. Interestingly, the encapsulated CuPOM/MOF composites in the presence of $H_2O_2$ demonstrate PMA > PTA ≈ STA ordering by antibacterial action, presumably reflecting their peroxidase-like catalytic activity [43].Since all tested POMs are strong acids, their actual acidity in the water medium is limited by the acidity of hydrated protons, and we may expect that the difference in POM antibacterial action is due to the redox properties of Keggin-type anions or their ability to penetrate the bacterial cell wall. Furthermore, the increase in silver solubility in the presence of POM may explain both the observed change in nanoparticle size caused by Ostwald ripening and the increase in antimicrobial action due to greater $Ag^+$ ions flux from the composite. Despite the differences in MIC, various POMs have in common better activity against Gram-negative bacteria. The structural difference between Gram-positive and Gram-negative bacteria causes the differences in the chemistry of formed biofilms and influences their interaction with nanoparticles [44]. It can be related to the thicker peptidoglycan layer in Gram-positive bacteria, which limits $H^+$ and $Ag^+$ diffusion into the cell, resulting in higher MICs [3].

We observed a significant improvement of antibacterial action when POM is supplemented with AgNPs, as HNT-POM composites without silver did not show any antibacterial action at 1.00 g/L dosage (data not shown). Despite the differences in particle size distribution, POM nature seems to be crucial in determining the antibacterial action, because HNT-Ag-PMA and HNT-Ag-PTA with broader AgNPs size distribution and larger average diameter have higher antibacterial activity than HNT-Ag and HNT-Ag-STA (see Fig. 2).

Although the HNT-Ag-PMA inhibits the growth of planktonic cells, MIC data are not sufficient to characterize the total antibacterial

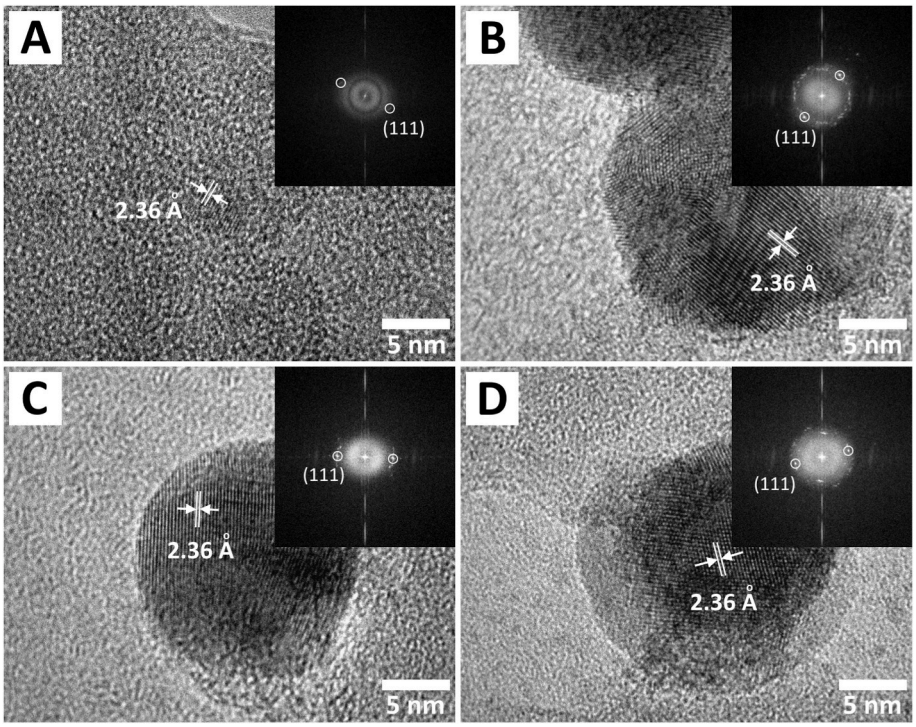



**Fig. 4.** HR-TEM of nanocomposites: HNT-Ag (A), HNT-PMA (B), HNT-PTA (C), HNT-STA (D) (scale bar is 5 nm). Insets show the Fourier transforms of the images with (111) signals indicated.

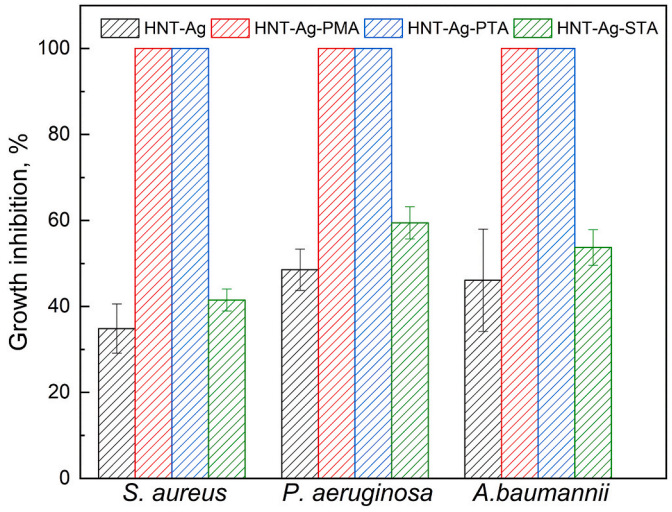



**Fig. 5.** Growth inhibition of *S. aureus, P. aeruginosa,* and *A. baumannii* planktonic cells by halloysite-based nanocomposites (1.00 g/L).

performance of nanocomposite. The ability of nanomaterials to combat already-formed biofilms is of great concern, and investigation of biofilm activity gives more relevant data about the antibacterial properties of the materials [45]. We decided to test the potential of HNT-Ag-PMA composite with better performance to deal with biofilms. We investigated the antibacterial activity associated with the destruction of formed biofilms (antibiofilm activity) at a nanocomposite concentration of 2.5 g/L (Fig. 6).

HNT-Ag-PMA reduces the viability of formed biofilms. Better antibiofilm performance is observed against Gram-negative bacteria. The reduction of biofilm viability up to four orders of magnitude indicates partial biofilm eradication by the composite as compared to untreated biofilms.

**Table 1**
MIC of HNT-Ag-PMA and HNT-Ag-PTA against planktonic bacteria.

| Organism | Composite | MIC, g/L | Reference |
|---|---|---|---|
| ***S. aureus*** | HNT-Ag-PMA | 0.50 | This work |
| ***P. aeruginosa*** | HNT-Ag-PMA | 0.25 | This work |
| ***A. baumannii*** | HNT-Ag-PMA | 0.25 | This work |
| ***S. aureus*** | HNT-Ag-PTA | 1.00 | This work |
| ***P. aeruginosa*** | HNT-Ag-PTA | 0.50 | This work |
| ***A. baumannii*** | HNT-Ag-PTA | 0.50 | This work |
| ***S. aureus*** | HNT-Ag-STA | >1.0[a] | This work |
| ***P. aeruginosa*** | HNT-Ag-STA | >1.0 | This work |
| ***A. baumannii*** | HNT-Ag-STA | >1.0 | This work |
| ***S. aureus*** | HNT-Ag | >1.0 | This work |
| ***P. aeruginosa*** | HNT-Ag | >1.0 | This work |
| ***A. baumannii*** | HNT-Ag | >1.0 | This work |
| ***S. aureus*** | AgNPs/PTA-PDA | >0.70 | [17] |
| ***E. coli*** | AgNPs/PTA-PDA | >0.70 | [17] |
| ***S. aureus*** | $Na_3[PMo_{12}O_{40}]\cdot nH_2O$ | 25.6 | [35] |
| ***E. coli*** | $H_3[PMo_{12}O_{40}]\cdot nH_2O$ | 3.92 | [36] |
| ***E. coli*** | Ag/PMA/RGO | 0.256 | [14] |
| ***S. aureus*** | Ag@GO | >0.10 | [37] |
| ***P. aeruginosa*** | Ag@GO | >0.10 | [37] |

[a] Values indicate the highest concentration tested; the complete growth inhibition was not observed.

## 4. Conclusions

In this work, we show a fast and simple routine to produce antibacterial halloysite-based nanocomposites with silver nanoparticles and polyoxometalates of Keggin structure. Although the nanoparticles formed on the nanocomposites have a broad size distribution, the obtained nanocomposites have dual-antibacterial performance acting on both Gram-positive *S. aureus* and Gram-negative *P. aeruginosa*, *A. baumannii.* The antibacterial action of the nanocomposites varies depending on the type of acid. The nanocomposite based on silver nanoparticles and phosphomolybdic acid has the best activity against planktonic bacterial cells, with MIC of 0.5 g/L for *S. aureus* and 0.25 g/L

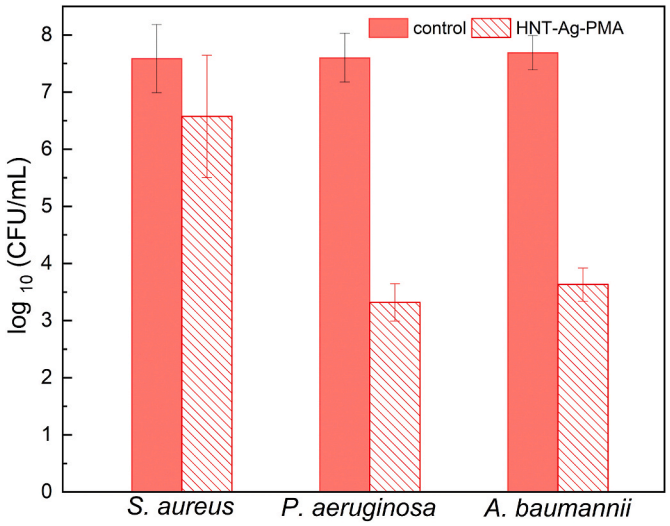



**Fig. 6.** Antibiofilm activity of HNT-Ag-PMA at 2.5 g/L.

for *P. aeruginosa* and *A. baumannii.* This composite also reduces the biofilm viability *P. aeruginosa* and *A. baumannii* for more than four orders of magnitude. The resulting nanocomposites can be used as a functional additive to paint compositions and as a component of smart coatings for protection against airborne and waterborne bacteria.

## Funding

The research was supported by the Russian Science Foundation (project No. 22-73-10224).

## Declaration of competing interest

The authors declare that they have no known competing financial interests or personal relationships that could have appeared to influence the work reported in this paper.

## Data availability

Data will be made available on request.

## Acknowledgments

The authors are grateful to N.N. Markelova from the Gause Institute of New Antibiotics (Moscow, Russia) for help in adapting the methodology of antibiofilm activity and for the generous gift of PTFE cubes.

## Appendix A. Supplementary data

Supplementary data to this article can be found online at https://doi.org/10.1016/j.jciso.2023.100098.

## References

[1] J. Sun, Z. Deng, A. Yan, Bacterial multidrug efflux pumps: mechanisms, physiology and pharmacological exploitations, Biochem. Biophys. Res. Commun. 453 (2014) 254–267, https://doi.org/10.1016/j.bbrc.2014.05.090.

[2] C. Adlhart, J. Verran, N.F. Azevedo, H. Olmez, M.M. Keinänen-Toivola, I. Gouveia, L.F. Melo, F. Crijns, Surface modifications for antimicrobial effects in the healthcare setting: a critical overview, J. Hosp. Infect. 99 (2018), https://doi.org/10.1016/j.jhin.2018.01.018.

[3] K.J. Woo, C.K. Hye, W.K. Ki, S. Shin, H.K. So, H.P. Yong, Antibacterial activity and mechanism of action of the silver ion in Staphylococcus aureus and Escherichia coli, Appl. Environ. Microbiol. 74 (2008) 2171–2178, https://doi.org/10.1128/AEM.02001-07.

[4] B.A. Bello, S.A. Khan, J.A. Khan, F.Q. Syed, M.B. Mirza, L. Shah, S.B. Khan, Anticancer, antibacterial and pollutant degradation potential of silver nanoparticles from Hyphaene thebaica, Biochem. Biophys. Res. Commun. 490 (2017) 889–894, https://doi.org/10.1016/j.bbrc.2017.06.136.

[5] J.R. Morones, J.L. Elechiguerra, A. Camacho, K. Holt, J.B. Kouri, J.T. Ramírez, M. J. Yacaman, The bactericidal effect of silver nanoparticles, Nanotechnology 16 (2005) 2346–2353, https://doi.org/10.1088/0957-4484/16/10/059.

[6] S. Feizi, C.M. Cooksley, G.S. Bouras, C.A. Prestidge, T. Coenye, A.J. Psaltis, P.-J. Wormald, S. Vreugde, Colloidal silver combating pathogenic Pseudomonas aeruginosa and MRSA in chronic rhinosinusitis, Colloids Surf. B Biointerfaces 202 (2021), 111675, https://doi.org/10.1016/j.colsurfb.2021.111675.

[7] A.A. Hamed, H. Kabary, M. Khedr, A.N. Emam, Antibiofilm, antimicrobial and cytotoxic activity of extracellular green-synthesized silver nanoparticles by two marine-derived actinomycete, RSC Adv. 10 (2020) 10361–10367, https://doi.org/10.1039/C9RA11021F.

[8] H.F. Hetta, I.M.S. Al-Kadmy, S.S. Khazaal, S. Abbas, A. Suhail, M.A. El-Mokhtar, N. H.A. Ellah, E.A. Ahmed, R.B. Abd-ellatief, E.A. El-Masry, G.E.S. Batiha, A. A. Elkady, N.A. Mohamed, A.M. Algammal, Antibiofilm and antivirulence potential of silver nanoparticles against multidrug-resistant Acinetobacter baumannii, Sci. Rep. 11 (2021) 1–11, https://doi.org/10.1038/s41598-021-90208-4.

[9] W. Zhou, Z. Jia, P. Xiong, J. Yan, Y. Li, M. Li, Y. Cheng, Y. Zheng, Bioinspired and biomimetic AgNPs/gentamicin-embedded silk fibroin coatings for robust antibacterial and osteogenetic applications, ACS Appl. Mater. Interfaces 9 (2017) 25830–25846, https://doi.org/10.1021/acsami.7b06757.

[10] H. Ishihama, K. Ishii, S. Nagai, H. Kakinuma, A. Sasaki, K. Yoshioka, T. Kuramoto, Y. Shiono, H. Funao, N. Isogai, T. Tsuji, Y. Okada, S. Koyasu, Y. Toyama, M. Nakamura, M. Aizawa, M. Matsumoto, An antibacterial coated polymer prevents biofilm formation and implant-associated infection, Sci. Rep. 11 (2021) 3602, https://doi.org/10.1038/s41598-021-82992-w.

[11] A. Bijelic, M. Aureliano, A. Rompel, The antibacterial activity of polyoxometalates: structures, antibiotic effects and future perspectives, Chem. Commun. 54 (2018) 1153–1169, https://doi.org/10.1039/c7cc07549a.

[12] K.B. S, V. Hemant, K. Daima, P.R. Selvakannan, Ahmad E. Kandjani, Ravi Shukla, 5 Bansal, Synergistic influence of polyoxometalate surface corona towards enhancing the antibacterial performance of tyrosine-capped Ag nanoparticles, Nanoscale 6 (2014) 758–765, https://doi.org/10.1039/c0xx00000x.

[13] L.P. Gonçalves, A. Miñán, G. Benítez, M.F.L. de Mele, M.E. Vela, P.L. Schilardi, E. P. Ferreira-Neto, J.C. Noveletto, W.R. Correr, U.P. Rodrigues-Filho, Self-sterilizing ormosils surfaces based on photo-synzthesized silver nanoparticles, Colloids Surf. B Biointerfaces 164 (2018), https://doi.org/10.1016/j.colsurfb.2017.12.016.

[14] M. Moghayedi, E.K. Goharshadi, K. Ghazvini, H. Ahmadzadeh, M.N. Jorabchi, Antibacterial activity of Ag nanoparticles/phosphomolybdate/reduced graphene oxide nanocomposite: kinetics and mechanism insights, Mater. Sci. Eng. B Solid-State Mater. Adv. Technol. 262 (2020), https://doi.org/10.1016/j.mseb.2020.114709.

[15] H. Haidari, R. Bright, S. Garg, K. Vasilev, A.J. Cowin, Z. Kopecki, Eradication of mature bacterial biofilms with concurrent improvement in chronic wound healing using silver nanoparticle hydrogel treatment, Biomedicines 9 (2021), https://doi.org/10.3390/biomedicines9091182.

[16] H. Soria-Carrera, E. Atrián-Blasco, J.M. de la Fuente, S.G. Mitchell, R. Martín-Rapún, Polyoxometalate-polypeptide nanoassemblies as peroxidase surrogates with antibiofilm properties, Nanoscale 14 (2022) 5999–6006, https://doi.org/10.1039/d1nr08223j.

[17] K. Zhou, Z. Zhang, J. Xue, J. Shang, D. Ding, W. Zhang, Z. Liu, F. Yan, N. Cheng, Hybrid Ag nanoparticles/polyoxometalate-polydopamine nano-flowers loaded chitosan/gelatin hydrogel scaffolds with synergistic photothermal/chemodynamic/Ag+ anti-bacterial action for accelerated wound healing, Int. J. Biol. Macromol. 221 (2022) 135–148, https://doi.org/10.1016/j.ijbiomac.2022.08.151.

[18] B. Díez, J. Santiago-Morales, M.J. Martínez-Bueno, A.R. Fernández-Alba, R. Rosal, Antimicrobial organic-inorganic composite membranes including sepiolite-supported nanometals, RSC Adv. 7 (2017) 2323–2332, https://doi.org/10.1039/c6ra26044f.

[19] D. Li, X. Gao, X. Huang, P. Liu, W. Xiong, S. Wu, F. Hao, H. Luo, Preparation of organic-inorganic chitosan@silver/sepiolite composites with high synergistic antibacterial activity and stability, Carbohydr. Polym. 249 (2020), 116858, https://doi.org/10.1016/j.carbpol.2020.116858.

[20] D. Peng, G. Liu, Y. He, P. Gao, S. Gou, J. Wu, J. Yu, P. Liu, K. Cai, Fabrication of a pH-responsive core–shell nanosystem with a low-temperature photothermal therapy effect for treating bacterial biofilm infection, Biomater. Sci. 9 (2021) 7483–7491, https://doi.org/10.1039/D1BM01329G.

[21] A. Stavitskaya, S. Batasheva, V. Vinokurov, G. Fakhrullina, V. Sangarov, Y. Lvov, R. Fakhrullin, Antimicrobial applications of clay nanotube-based composites, Nanomaterials 9 (2019) 708, https://doi.org/10.3390/nano9050708.

[22] W. Wei, R. Minullina, E. Abdullayev, R. Fakhrullin, D. Mills, Y. Lvov, Enhanced efficiency of antiseptics with sustained release from clay nanotubes, RSC Adv. 4 (2014) 488–494, https://doi.org/10.1039/c3ra45011b.

[23] E. Abdullayev, K. Sakakibara, K. Okamoto, W. Wei, K. Ariga, Y. Lvov, Natural tubule clay template synthesis of silver nanorods for antibacterial composite coating, ACS Appl. Mater. Interfaces 3 (2011), https://doi.org/10.1021/am200896d.

[24] Y.M. Lvov, D.G. Shchukin, H. Möhwald, R.R. Price, Halloysite clay nanotubes for controlled release of protective agents, ACS Nano 2 (2008) 814–820, https://doi.org/10.1021/nn800259q.

[25] K. Cherednichenko, D. Kopitsyn, S. Batasheva, R. Fakhrullin, Probing antimicrobial halloysite/biopolymer composites with electron microscopy: advantages and limitations, Polymers (Basel) 13 (2021) 3510, https://doi.org/10.3390/polym13203510.

[26] A.A. Novikov, A.R. Sayfutdinova, M.V. Gorbachevskii, S.V. Filatova, A. V. Filimonova, U.P. Rodrigues-Filho, Y. Fu, W. Wang, H. Wang, V.A. Vinokurov, D. G. Shchukin, Natural nanoclay-based silver-phosphomolybdic acid composite with a dual antimicrobial effect, ACS Omega 7 (2022) 6728–6736, https://doi.org/10.1021/acsomega.1c06283.

[27] V.S. Sadykova, I.A. Gavryushina, A.E. Kuvarina, N.N. Markelova, N.G. Sedykh, M. L. Georgieva, A.C. Barashkova, E.A. Rogozhin, Antimicrobic activity of the lipopeptide emericellipsin A isolated from emericellopsis alkalina against biofilm-forming bacteria, Appl. Biochem. Microbiol. 56 (2020) 292–297, https://doi.org/10.1134/S0003683820030102.

[28] L. Lee, J.X. Wang, R.R. Adžić, I.K. Robinson, A.A. Gewirth, Adsorption configuration and local ordering of silicotungstate anions on Ag(100) electrode surfaces, J. Am. Chem. Soc. 123 (2001) 8838–8843, https://doi.org/10.1021/ja0161352.

[29] S. Sharet, E. Sandars, Y. Wang, O. Zeiri, A. Neyman, L. Meshi, I.A. Weinstock, Orientations of polyoxometalate anions on gold nanoparticles, Dalton Trans. 41 (2012) 9849–9851, https://doi.org/10.1039/c2dt30592e.

[30] G.M. Maksimova, A.L. Chuvilin, E.M. Moroz, V.A. Likholobov, K.I. Matveev, Preparation of colloidal solutions of noble metals stabilized by polyoxometalates and supported catalysts based on these solutions, Kinet. Catal. 45 (2004) 870–878, https://doi.org/10.1007/s10975-005-0054-3.

[31] A. Dolbecq, J.D. Compain, P. Mialane, J. Marrot, F. Sécheresse, B. Keita, L.R. B. Holzle, F. Miserque, L. Nadjo, Hexa- and dodecanuclear polyoxomolybdate cyclic compounds: application toward the facile synthesis of nanoparticles and film electrodeposition, Chem. Eur J. 15 (2009) 733–741, https://doi.org/10.1002/chem.200800719.

[32] Y.B. Matos, R.S. Romanus, M. Torquato, E.H. de Souza, R.L. Villanova, M. Soares, E.R. Viana, Silver nanoparticles nucleated in NaOH-treated halloysite: a potential antimicrobial material, Beilstein J. Nanotechnol. 12 (2021), https://doi.org/10.3762/bjnano.12.63.

[33] R.W. Korsmeyer, N.A. Peppas, Effect of the morphology of hydrophilic polymeric matrices on the diffusion and release of water soluble drugs, J. Membr. Sci. 9 (1981), https://doi.org/10.1016/S0376-7388(00)80265-3.

[34] J. Hasan, Y. Xu, T. Yarlagadda, M. Schuetz, K. Spann, P.K.D.V. Yarlagadda, Antiviral and antibacterial nanostructured surfaces with excellent mechanical properties for hospital applications, ACS Biomater. Sci. Eng. 6 (2020), https://doi.org/10.1021/acsbiomaterials.0c00348.

[35] T. Yamase, N. Fukuda, Y. Tajima, Synergistic effect of polyoxotungstates in combination with β-lactam antibiotics on antibacterial activity against methicillin-resistant Staphylococcus aureus, Biol. Pharm. Bull. (1996), https://doi.org/10.1248/bpb.19.459.

[36] M. Moghayedi, E.K. Goharshadi, K. Ghazvini, H. Ahmadzadeh, R. Ludwig, M. Namayandeh-Jorabchi, Improving antibacterial activity of phosphomolybdic acid using graphene, Mater. Chem. Phys. (2017), https://doi.org/10.1016/j.matchemphys.2016.12.037.

[37] N.T.H. Nam, N.M. Dat, N.D. Hai, L.M. Huong, L.T. Tai, N.T. Dat, H. An, P.N. P. Hung, N.T. Truong, N.T. Son, M.T. Phong, N.H. Hieu, Green synthesis of silver@graphene oxide nanocomposite for antibacterial, cytotoxicity assessment, and hydrogen peroxide electro-sensing, New J. Chem. (2023) 8090–8101, https://doi.org/10.1039/d3nj00618b.

[38] M.J. Da Silva, D.M. Chaves, A.A. Júlio, F.A. Rodrigues, C.G.O. Bruziquesi, Sn(II)-Exchanged Keggin silicotungstic acid-catalyzed etherification of glycerol and ethylene glycol with alkyl alcohols, Ind. Eng. Chem. Res. 59 (2020) 9858–9868, https://doi.org/10.1021/acs.iecr.0c00229.

[39] L. Shen, H. Yin, A. Wang, Y. Feng, Y. Shen, Z. Wu, T. Jiang, Liquid phase dehydration of glycerol to acrolein catalyzed by silicotungstic, phosphotungstic, and phosphomolybdic acids, Chem. Eng. J. 180 (2012) 277–283, https://doi.org/10.1016/j.cej.2011.11.058.

[40] Ștefana Bălici, D. Rusu, E. Páll, M. Filip, F. Chirilă, G.Z. Nicula, M.L. Vică, R. Ungur, H.V. Matei, N.I. Fiț, In vitro antibacterial susceptibility of different pathogens to thirty nano-polyoxometalates, Pharmaceuticals 15 (2021) 33, https://doi.org/10.3390/ph15010033.

[41] I.V. Kozhevnikov, Heterogeneous acid catalysis by heteropoly acids: approaches to catalyst deactivation, J. Mol. Catal. Chem. 305 (2009) 104–111, https://doi.org/10.1016/j.molcata.2008.11.029.

[42] A. Alasmari, R. Al-Faze, E.F. Kozhevnikova, I.V. Kozhevnikov, Solid acid catalysts comprising heteropoly acids supported on SiO2, TiO2 and ZrO2: a microcalorimetric investigation of catalyst acidity and new insight into the mechanism of alcohol dehydration over HPA, Catal. Commun. 180 (2023), 106710, https://doi.org/10.1016/j.catcom.2023.106710.

[43] L. Zhu, A. Huo, Y. Chen, X. Bai, C. Cao, Y. Zheng, W. Guo, A ROS reservoir based on a polyoxometalate and metal-organic framework hybrid for efficient bacteria eradication and wound healing, Chem. Eng. J. 476 (2023), 146613, https://doi.org/10.1016/j.cej.2023.146613.

[44] W. Pajerski, D. Ochonska, M. Brzychczy-Wloch, P. Indyka, M. Jarosz, M. Golda-Cepa, Z. Sojka, A. Kotarba, Attachment efficiency of gold nanoparticles by Gram-positive and Gram-negative bacterial strains governed by surface charges, J. Nanoparticle Res. 21 (2019) 186, https://doi.org/10.1007/s11051-019-4617-z.

[45] A.M. Ferreira, A. Vikulina, G.W.V. Cave, M. Loughlin, V. Puddu, D. Volodkin, Vaterite vectors for the protection, storage and release of silver nanoparticles, J. Colloid Interface Sci. 631 (2023) 165–180, https://doi.org/10.1016/j.jcis.2022.10.094.